JAERI-M
88-207

MHD EQUILIBRIUM CALCULATIONS SPECIFYING CURRENT SOURCES

October 1988

Shinji TOKUDA, Tatsuoki TAKEDA
and Masao OKAMOTO*

日本原子力研究所
Japan Atomic Energy Research Institute

編集兼発行　日本原子力研究所
印　　刷　山田軽印刷所

MHD Equilibrium Calculations Specifying Current Sources

Shinji TOKUDA, Tatsuoki TAKEDA
and Masao OKAMOTO*

Department of Thermonuclear Fusion Research
Naka Fusion Establishment
Japan Atomic Energy Research Institute
Naka-machi, Naka-gun, Ibaraki-ken

(Received September 26, 1988)

A MHD equilibrium code in which current sources are specified instead of toroidal field function or safety factor has been developed. This code is appropriate to self-consistent analysis of neoclassical current effects (bootstrap current and neoclassical conductivity) in the plasma sustained by the ohmic current. The code can be also applied to equilibrium and stability analysis of tokamak plasmas with non-ohmic currents driven by external sources (NBI/RF-wave) and with neoclassical current effects.

Keywords: MHD Equilibrium, Bootstrap Current, Ohmic Current, Neoclassical Conductivity, Tokamak

---

* Institute of Plasma Physics, Nagoya University

電流源が与えられたMHD平衡計算

日本原子力研究所那珂研究所核融合研究部
徳田　伸二・竹田　辰興・岡本　正雄*

（1988年9月26日受理）

トロイダル磁場関数や安全係数の代わりに，電流源を与えてＭＨＤ平衡を求めるコードを開発した。このコードは，オーム電流で維持されたプラズマ中での新古典電流効果（ブートストラップ電流及び新古典電導率）の無矛盾な解析に有効である。また，このコードは外部源（ＮＢＩ／ＲＦ－wave）で駆動される非オーム電流及び新古典電流効果のあるトカマク・プラズマの平衡・安定性解析に応用することができる。

那珂研究所：〒311－01　茨城県那珂郡那珂町大字向山801－1
＊　名古屋大学プラズマ研究所

Contents

目　　次

1. Introduction

Calculation of MHD equilibria of tokamak plasmas is the first step of both theoretical and experimental research of controlled thermonuclear fusion by tokamaks. It is necessary for MHD stability and confinement studies, and is also indispensable for design of tokamak devices. Therefore various numerical methods of computing MHD equilibria of tokamak plasmas have been devised and many equilibrium code have been developed to use for the particular purpose mentioned above [1,2,3,4,5,6].

MHD equilibrium in axisymmetric toroidal configurations such as tokamaks are described by a semi-linear elliptic partial differential equation for the poloidal flux function ψ known as the Grad-Shafranov equation. This equation has two source terms : the pressure p and the toroidal field function F , both of which are functions of only ψ . Solving the equation requires specifying p and F with appropriate boundary conditions. The equation can be also solved by specifying the safety factor instead of F according to the flux conserving tokamak (FCT) algorithm [7]. With this algorithm high beta equilibria are easily computed. It is widely used in MHD stability analysis because the safety factor which plays an important role in the stability theory is prescribed. However neither toroidal field function nor safety factor are quantities measured directly in tokamak experiments. Therefore in MHD analysis of experiments the function F is fitted, for example, by using polynomials to reproduce the magnetic data in many equilibrium codes [8].

For confinement of a tokamak plasma the toroidal current must be supplied by external sources. The transport theory shows that the current sources produce the surface average parallel current. Generalized Ohm's law relates the parallel current to the inductive electric field driving the ohmic current and to pressure/temperature gradients (thermodynamic forces) [9,10,11]. The currents driven by non-ohmic external sources (NBI/RF wave) are also given as the surface average parallel current [10,11]. Therefore calculating MHD equilibria by specifying the current sources (surface averaged parallel currents) together with generalized Ohm's law may be considered to provide a useful means for theoretical/experimental study of confinement of tokamak plasmas. It enables to compute MHD equilibria sustained by the ohmic current from only measured quantities such as density/temperature profiles, one-turn voltage and effective Z (Z_{eff}) without using the ambiguous quantities F. It also enables the self-consistent study of neoclassical current effects on MHD equilibria (bootstrap current and neoclassical conductivity), which get renewed attention recently [12,13], and that of a steady tokamak sustained by non-ohmic currents with the help of appropriate current-drive theory [14,15,16].

The paper is organized as follows: the basic equations for tokamak MHD equilibria specified the current sources are derived in Section 2. In Section 3, a numerical scheme to solve them self-consistently is presented. The scheme is applied to high aspect ratio circular tokamaks to validate it in Section 4 and summary is given in Section 5. SI unit is used throughout this paper except temperature measured in ev.

2. Basic Equations

2.1 Parallel Current In a Tokamak Plasma

In an axisymmetric toroidal configuration such as tokamaks, equilibrium magnetic field $\boldsymbol{B}$ is represented by a stream function (poloidal flux function) ψ as

$$\boldsymbol{B} = \nabla\phi \times \nabla\psi + F\nabla\phi \quad , \qquad (1)$$

and $F = RB_t$ (B_t : toroidal magnetic filed) is the toroidal field function. Here the usual cylindrical coordinate system (R, Z, ϕ) is employed. Force balance equation, $\nabla p = \boldsymbol{J} \times \boldsymbol{B}$, yields a second order elliptic partial differential equation, known as the Grad-Shafranov equation (μ_0 : permeability of vacuum) [1,2] :

$$\Delta^*\psi = R\,\mu_0 j_\phi \quad , \qquad (2)$$

with

$$\Delta^*\psi = \frac{\partial^2\psi}{\partial R^2} + \frac{\partial^2\psi}{\partial Z^2} - \frac{1}{R}\frac{\partial\psi}{\partial R} \ . \qquad (3)$$

The toroidal current j_ϕ is given by

$$Rj_\phi = -R^2\frac{dp}{d\psi} - \frac{1}{\mu_0}F\frac{dF}{d\psi} \quad , \qquad \textit{in plasma}, \qquad (4)$$

$$Rj_\phi = 0 \quad , \qquad \textit{in vacuum},$$

and F and pressure p are functions of only ψ. To solve Eqs.(2) and (4) the functions, p and T, have to be specified with appropriate boundary conditions. The equations can be solved by specifying the safety factor

$$q(\psi) = \frac{F}{2\pi}\int\frac{dl}{R^2 B_p} \ , \qquad (5)$$

by using the flux conserving tokamak algorithm [7]. Here B_p is the poloidal filed and dl the line element of the contour line of $\psi = const.$ Many equilibrium codes so far solve the Grad-Shafranov equation by giving the pair (p, F) or (p, q). However neither the toroidal function F nor safety factor q are quantities measured directly in experiments. Transport theory shows that the surface average parallel current is related directly to measurable quantities such as the inductive electric field, density and temperature.

The current in an equilibrium plasma is

$$\boldsymbol{J} = \boldsymbol{J}_{\perp} + J_{//}\boldsymbol{B}/B \ , \tag{6}$$

$$\boldsymbol{J}_{\perp} = \boldsymbol{B} \times \nabla p/B^2 \ , \tag{7}$$

and the parallel current

$$J_{//} = -\frac{F}{B}\frac{dp}{d\psi} - \frac{1}{\mu_0}\frac{dF}{d\psi}B \ , \tag{8}$$

can be rewritten as

$$J_{//} = -\frac{F}{B}\frac{dp}{d\psi}\left[1 - \frac{B^2}{\langle B^2\rangle}\right] + \frac{\langle j \cdot B\rangle}{\langle B^2\rangle}B \ . \tag{9}$$

Here $\langle X\rangle$ denotes the flux surface average [9] :

$$\langle X\rangle = \int \frac{X}{B_p}dl \Big/ \int \frac{1}{B_p}dl = \int_0^{2\pi} \sqrt{g}\,X d\theta \Big/ \int_0^{2\pi} \sqrt{g}\,d\theta \ , \tag{10}$$

with θ being the poloidal angle of a flux coordinate system (ψ, θ, ϕ) and

$$\sqrt{g} = [(\nabla\psi \times \nabla\theta) \cdot \nabla\phi]^{-1} \ . \tag{11}$$

The first term of Eq.(9) is the Pfirsh-Schlüter return current which flows automatically to maintain the charge neutrality condition on each flux surface and the second term, which is divergence-free, is a unidirectional parallel current necessary to maintain the equilibrium parallel momentum balance along the magnetic field [17]. For confinement of tokamak plasmas this current must be supplied by external sources. Equations (8) and (9) give the equation for $FdF/d\psi$ represented by the pressure and surface average parallel current :

$$F\frac{dF}{d\psi} = -\mu_0 [\frac{F^2}{<B^2>}\frac{dp}{d\psi} + F\frac{<J\cdot B>}{<B^2>}] . \tag{12}$$

Therefore the Grad-Shafranov equation can be solved by specifying the surface average parallel current $<\boldsymbol{J}\cdot\boldsymbol{B}>$ with the pressure ; in this method the function F is obtained by solving the ordinary differential equation, Eq.(12). From Eqs.(6), (7) and (9) the toroidal current j_ϕ reads :

$$j_\phi = Rj\cdot\nabla\phi = -R\frac{dp}{d\psi}[1 - \frac{B_t^2}{<B^2>}] + \frac{<J\cdot B>}{<B^2>}B_t . \tag{13}$$

2.2 Generalized Ohm's Law

The flux surface average parallel currents are determined by the thermodynamic forces (electric filed and pressure/temperature gradients) according to the neoclassical transport theory [10,11] :

$$<J\cdot B> = <J\cdot B>_E + <J\cdot B>_B + <J\cdot B>_S , \tag{14}$$

where $<\boldsymbol{J}\cdot\boldsymbol{B}>_E$ is the ohmic current, $<\boldsymbol{J}\cdot\boldsymbol{B}>_B$ the bootstrap current and $<\boldsymbol{J}\cdot\boldsymbol{B}>_S$ stands for non-ohmic currents driven by external sources. The ohmic current is driven by the inductive electric filed :

$$<J\cdot B>_E = \sigma_{NC}<B\cdot E> = \frac{n_e e^2 \tau_{ee}}{m_e}\Lambda_{NC}<E\cdot B>, \tag{15}$$

where σ_{NC} is the neoclassical conductivity which reduces to the classical Spitzer conductivity (Z_I: charge number of the ion)

$$\sigma_{Spitzer} = \frac{n_e e^2 \tau_{ee}}{m_e Z_I}\frac{3.25Z_I^2 + 1.41Z_I}{Z_I^2 + 1.41Z_I} . \tag{16}$$

when the trapped particle effects are not considered. In Eq.(15) τ_{aa} $(a=e,i)$ is the Braginskii Coulomb collision time :

$$\frac{1}{\tau_{aa}} = \frac{4}{3\sqrt{\pi}} \frac{n_a e_a^4}{m_a v_{ta}^3} \frac{\ln\Lambda}{4\pi\varepsilon_0^2}, \tag{17}$$

v_{ta} the thermal velocity defined by $v_{ta} = \sqrt{2T_a/m_a}$ and $\ln\Lambda$ the Coulomb logarithm (ε_0 : permittivity of vacuum). Other notations are standard. For a plasma in a stationary state, the flux surface average parallel electric field $<\boldsymbol{E}\cdot\boldsymbol{B}>$ is expressed by the one-turn voltage V_L [18]:

$$<\boldsymbol{E}\cdot\boldsymbol{B}> = <\boldsymbol{B}\cdot\nabla\phi> V_L/2\pi\ . \tag{18}$$

The non-ohmic currents $<\boldsymbol{J}\cdot\boldsymbol{B}>_S$ may be computed from the distribution function of electrons or fast ions given by the theories on current drive [15,19]. The bootstrap current is expressed as [11]

$$<\boldsymbol{J}\cdot\boldsymbol{B}>_B = -F\, p_e(L^e{}_{31}A_p + L^e{}_{32}A_{Te} + L^i{}_{32}A_{Ti}), \tag{19}$$

$$A_p = \frac{d}{d\psi}\ln p_e + \frac{T_i}{Z_I T_e}\frac{d}{d\psi}\ln p_i\,,$$

$$A_{Te} = \frac{d}{d\psi}\ln T_e\,,\ A_{Ti} = \frac{T_i}{Z_I T_e}\frac{d}{d\psi}\ln T_i\,, \tag{20}$$

where $p_a = 1.60\times10^{-19}\, n_a T_a\ (a = e,\ i)$. The coefficients $L^e{}_{31}$, $L^e{}_{32}$ and $L^i{}_{32}$ as well as Λ_{NC}, are expressed by the dimensionless friction matrix elements $l_{ij}{}^a$ and the dimensionless viscosity matrix $[\mu^a]$:

$$[\mu^a] = \begin{pmatrix} \mu_1{}^a & \mu_2{}^a \\ \mu_2{}^a & \mu_3{}^a \end{pmatrix} .$$

Their explicit expressions are :

$$L^e{}_{31} = \quad [\mu_1{}^e(\mu_3{}^e + l_{22}{}^e) - \mu_2{}^e(l_{12}{}^e + \mu_2{}^e)]/D ,$$

$$L^e{}_{32} = \quad (\mu_3{}^e\, l_{12}{}^e \; - \mu_2{}^e l_{22}{}^e)/D ,$$

$$L^i{}_{32} = \quad -L_{31}{}^e l_{22}{}^i\, \mu_2{}^i\, [\mu_1 i\, (\mu_3 i + l_{22}{}^i) - (\mu_2{}^i)^2] , \qquad (21)$$

$$\Lambda_{NC} = (\mu_3{}^e + l_{22}{}^e)/D ,$$

$$D = (\mu_1{}^e + l_{11}{}^e)(\mu_3{}^e + l_{22}{}^e) - (\mu_2{}^e + l_{12}{}^e)^2 .$$

The viscosity matrix $[\mu^a]$ $(a = e, i)$ is computed from the positive definite matrix $[K^a]$ * :

$$\mu_1 = K_{11},$$
$$\mu_2 = 5/2 \;\; K_{11} - K_{12} , \qquad (22)$$
$$\mu_3 = 25/4 \; K_{11} - 5\, K_{12} + K_{22} .$$

The matrix elements K_{ij} valid in all collisionality regimes and arbitrary plasma cross section can be obtained approximately by a rational combination of its asymptotic forms in various collisionality regimes [10,11] :

* We omit the superscript "a" denoting the species hereafter

$$K_{ij} = \frac{g_t K_{ij}{}^B}{(1+2.92\nu_* \frac{1}{\omega_{ta}\tau_{aa}} \frac{K_{ij}{}^B}{K_{ij}{}^P})(1+\frac{1}{6\omega_{ta}\tau_{aa}} \frac{K_{ij}{}^P}{K_{ij}{}^{PS}})} . \qquad (23)$$

Here g_t is the ratio of the average fraction of trapped particles to that of circulating particles :

$$g_t = f_t/f_c , \qquad (24)$$

$$f_c = \frac{3<B^2>}{4(B_{max})^2} \int_0^1 \frac{\lambda d\lambda}{< \sqrt{1-\lambda B/B_{max}} >} . \qquad (25)$$

The quantities ω_{ta} is the average transit frequency of the species a defined by [20]

$$\omega_{ta} = v_{ta} < \frac{1}{\sqrt{g}B} > \approx \frac{v_{ta}}{R_0 q} , \qquad (26)$$

where R_0 is the position of the magnetic axis. The collisional parameter ν_* is given by

$$\nu_* = \frac{g_t}{2.92} < \frac{1}{\sqrt{g}B} > \frac{<B^2>}{<(\mathbf{B}\cdot\nabla B/B)^2>} . \qquad (27)$$

The matrices K^B, K^P and K^{PS} for electrons and ions are given in ref.[11] and summarized in Table 1 with the friction matrix elements $l_{ij}{}^a$. The three collisional regimes for each species can be seen from Eq.(23) :

Pfirsh-Schlüter regime : $\frac{1}{\omega_{ta}\tau_{aa}} \gg 1$,

Plateau regime : $\frac{1}{\nu^*} \ll \frac{1}{\omega_{ta}\tau_{aa}} \ll 1$, (28) Banana regime : $\frac{1}{\omega_{ta}\tau_{aa}} \ll \frac{1}{\nu^*}$.

Equations (2), (4), (12) and (14) form the basic equations for MHD equilibria specified the current sources. Equations (19) and (20) make it possible to evaluate self-consistently the neoclassical effects on tokamak plasmas with finite aspect ratio, arbitrary cross section for all collisional regimes. By being composed with the theories on current drive, equilibria in a steady state with the non-ohmic currents and the neoclassical effects can be calculated .

3. Numerical Scheme

The basic equations are solved numerically by iteration for prescribed density and temperature given as functions of normalized Ψ ($\Psi = (\psi_{axis} - \psi)/\psi_{axis}$) . Z_{eff} is assumed to be uniform for simplicity. The Cartetian coordinate is implemented. The partial differential equation, Eq.(2), is solved in a computational box which contains the plasma (Fig.1). At each iteration step vacuum field solutions (solutions of $\Delta^* \psi = 0$) are added to the solution of Eq.(2) so that the plasma surface ($\psi = 0$) may pass the specified fixed points (semi-fixed boundary method). Analytical vacuum field solutions are used, which are expressed by the associated Legendre polynomials. The boundary values are loaded on Γ through Green's theorem :

$$\psi(R,Z) = \int G(R, Z : R^*, Z^*) Bp(R^*, Z^*) dl, \tag{29}$$

where $G(R, Z : R^*, Z^*)$ is the Green function of the operator Δ^* [2] and dl is the line element of the contour line of $\psi = 0$. Equation (5) is approximated by standard 5-points finite-differences and the boundary value problem of Dirichlet type is solved by Double Cyclic Reduction(DCR) method [21] ; the number of grid points of R and Z must be $2^N + 1$. The toroidal current j_ϕ is loaded on the (R,Z) grids , according to Eqs.(4) and (12), from $dp/d\psi$ and $FdF/d\psi$ assigned on the ψ grids by using a linear interpolation.

On solving Eq.(2), the constraint that the total toroidal current I_p takes the given value is imposed. For a plasma sustained by the ohmic current, the constraint reads

$$I_p = I_{ps} + I_{ohm} + I_{BS} = given \quad , \tag{30}$$

$$I_{ps} = -\frac{1}{2\pi}\int \frac{dp}{d\psi}\frac{<B_p{}^2>}{<B^2>}dV, \tag{31.a}$$

$$I_{ohm} = \frac{1}{2\pi}\frac{V_L}{2\pi}\int \sigma_{NC} < \frac{1}{R^2} > \frac{<B_t{}^2>}{<B^2>}dV, \tag{31.b}$$

$$I_{BS} = \frac{1}{2\pi}\int \frac{<\boldsymbol{J}\,\boldsymbol{B}>_{BS}}{<B^2>}F < \frac{1}{R^2} > dV. \tag{31.c}$$

The one-turn voltage V_L is determined such that Ip may be equal to the prescribed value, and then the parallel current is updated to compute $FdF/d\psi$ for next iteration through Eq.(12). For a plasma with the externally driven current, the strength of the source (power of NBI/RF wave) is determined from the constraint.

On computing bootstrap current and neoclassical conductivity, several surface average quantities are needed. To obtain them we construct the flux coordinate system (ψ,θ,ϕ) where the poloidal angle θ and $\sqrt{g}$ are

$$\theta = \frac{2\pi}{L}\int_0 dl, \tag{32}$$

$$\sqrt{g} = \frac{L}{2\pi B_p} \; . \tag{33}$$

Here L is the total length of the contour line, ψ = *const.* . In a flux coordinate system, $<(\boldsymbol{B}\cdot\nabla B/B)^2>$, for example, is expressed as

$$< (\frac{\boldsymbol{B}\cdot\nabla B}{B})^2 > = \frac{\displaystyle\int_0^{2\pi}(\partial_\theta B/B)^2/\sqrt{g}\,d\theta}{\displaystyle\int_0^{2\pi}\sqrt{g}\,d\theta} \; . \tag{34}$$

We obtain poloidal angle θ and a quantity X on each flux surface when drawing a contour line. We interpolate X onto uniform spacing θ grids with periodic spline functions. We can compute the values of $dX/d\theta$ as well as X on the uniform grids of θ. The trapezoid formula is used in integrating along the θ coordinate.

The integrand of Eq.(25) becomes singular when $\lambda = 1$. To get numerical accuracy the independent variable λ is transformed to μ by

$$\lambda = \tanh\mu \qquad (0 \le \mu \le \mu_{max}), \tag{35}$$

and trapezoid formula is employed for integraing Eq.(25).

The initial solutions of ψ and F are the Solov'ev equilibrium [22] and the value of F in the vacuum region. The iteration is terminated when the changes in the solutions ψ, $FdF/d\psi$ and V_L are smaller than a desired tolerance δ:

$$\begin{aligned} &\|\psi^{n+1} - \psi^n\| < \delta, \\ &\|(FdF/d\psi)^{n+1} - (FdF/d\psi)^n\| < \delta, \\ &|V_L{}^{n+1} - V_L{}^n| < \delta, \end{aligned} \tag{36}$$

where superscript n denotes the number of iterations and $\|f(x)\| = \max|f(x)|$.

4. Results for High Aspect Ratio Circular Tokamaks

The numerical scheme is applied to high aspect ratio circular tokamaks (HARCT) with the ohmic currents to validate it. The parameters of the plasma are : the major radius $R_{maj} = 1.0\ m$, the minor radius $a = 0.2\ m$, the vacuum toroidal filed at the plasma center $B_{t0} = 4\ T$ and the total toroidal current $I_p = 200kA$. These parameters yield equilibria with $q_a \approx 4$ for $\beta_J << 1$, where q_a is the safety factor at the plasma edge and β_J is the poloidal beta defined by $\beta_J = \int p dV/(R_{maj}\mu_0 I_P{}^2)$. The hydrogen plasma ($Z_{eff} = 1$) with $T_e(\Psi) = T_i(\Psi)$ is assumed for simplicity (Ψ : normalized ψ). The profiles of density and temperature are given by the function (f stands for density, n, or temperature, T)

$$\frac{df}{d\Psi} = -C\,(\Psi - \Psi_d)^{\alpha}(1-\Psi)\,. \tag{37}$$

Here Ψ_d is so determined that the peak position Ψ_p of the profile takes the prescribed value and C is computed from the values of f at the magnetic axis, f_0, and at the plasma edge, f_a . For the present case $\Psi_p = 0.49$, $\alpha = 2$, $n_0 = 1.75 \times 10^{20}\ m^{-3}$, $n_a = 1.75 \times 10^{18}\ m^{-3}$, $T_0 = 2kev$ and $T_a = 20\ ev$.

The number of grids points on the (R,Z) coordinates are $N_R \times N_Z = 513 \times 257$; for the flux coordinates $N\psi \times N_\theta = 41 \times 81$; μ_{max} in Eq.(35) is 6 and the number of points for the numerical quadrature is $N_\mu = 101$; $\delta = 10^{-4}$ is taken as the tolerance in Eq.(36).

In HARCT limit, f_t and $\nu*$ at the radius r can be approximated as

$$f_t = 1.46\sqrt{\varepsilon}\,, \tag{38}$$

$$\nu* = \varepsilon^{-3/2}(1-1.46\sqrt{\varepsilon})\,, \tag{39}$$

with $\varepsilon = r/R_0$. Figure 2 shows f_t and ν_*^{-1} computed from the code (solid lines) and from the Eqs.(38) and (39) (dotted lines). The agreement between them is excellent for $\varepsilon \leq 0.1$. The code yields the correct behavior of f_t and ν_*^{-1} near the magnetic axis. In Fig.3 the neoclassical current coefficients, $L^e{}_{31}$, $L^e{}_{32}$ and $L^i{}_{32}$, (Fig.3(a)) and Λ_{NC} (Fig.3(b)) are shown as functions of Ψ (solid lines). The HARCT limits are also shown for comparison by dotted lines. The agreement is again excellent. The transition region between the banana regime and the plateau regime is near $\Psi \approx 0.65$ for the present case (the region near the magnetic axis is intrinsically in Pfirsch-Schlüter and plateau regimes). Smooth transition of the coefficients from the banana regime to the plateau regime is obtained. The coefficients, $L^e{}_{32}$ and $L^i{}_{32}$ have negative values and same order absolute values to $L^e{}_{31}$, which means that the bootstrap current is mainly driven by the density gradient. The neoclassical conductivity (Fig.3(b)) is about $60 \sim 70\%$ of the Spitzer conductivity in the almost regions. When Ψ approaches to the magnetic axis the conductivity tends to $\sigma_{Spitzer}$ rapidly due to mainly disappearance of trapped particles. Figures 2(a) and 3(b) indicate that it is important to take account of the finite aspect ratio effect for $A < 5$. The HARCT approximation, Eq.(38), overestimates f_t and underestimates σ_{NC}. This will cause errors in the estimation of Z_{eff} in the analyses of MHD equilibria of tokamak experiments.

Figures 4 and 5 illustrate contour lines and toroidal currents in the midplane ($Z = 0$) of the equilibrium without neoclassical current effects (classical equilibrium) and with the neoclassical effects (neoclassical equilibrium), respectively : for the classical equilibrium, $I_{ohm} = 199.0\ kA$, $I_{ps} = 1.0\ kA$, $V_L = 0.417\ volt$, $\beta_J =$

1.52, $\psi_{axis} = -4.15 \times 10^{-2}$ *weber*, $q_0 = 1.0$ and $q_a = 4.55$; for the neoclassical equilibrium, $I_{ohm} = 96.3\ kA$, $I_{BS} = 102.8\ kA$, $I_{ps} = 0.9\ kA$, $V_L = 0.275$ *volt*, $\beta_J = 1.77$, $\psi_{axis} = -3.54 \times 10^{-2}$ *weber*, $q_0 = 1.5$ and $q_a = 4.60$. The broad current profile of the neoclassical equilibrium produces the contour lines enclosing larger volumes than those of the classical equilibrium and then higher β_J, higher q_0 and a smaller value of ψ_{axis}.

The neoclassical current effects cause different current profiles from those of the classical equilibrium. The ohmic current for the neoclassical equilibrium (dotted line in Fig.5(b)) has a peaked profile in accordance with the profile of σ_{NC} in Fig.3(b). The value of I_{ohm} for it is about half of that for the classical equilibrium but the one-turn voltage does not reduce so much due to the reduction of the conductivity. The bootstrap current has a hollow profile which is one of the typical features of the neoclassical equilibria. The large bootstrap current and the reduced ohmic current give rise to the safety factor with a high q_0 and a flat q profile (Fig.6). It is seen from broken lines in Figs.4(b) and 5(b) that the pressure contributions to the toroidal currents, the first term of Eq.(13), show the typical feature of return currents ; it is positive for $R > R_0$ and negative for $R < R_0$ (R_0 : position of the magnetic axis). Volume integration of them almost cancel to remain small diamagnetic currents.

5. Summary

A numerical scheme for self-consistent calculations of MHD equilibria specified current sources has been presented. The scheme employs the surface averaged parallel current on computing equilibria instead of the toroidal field function or safety factor. The scheme has been applied to high aspect ratio circular tokamaks with the ohmic current. It has been shown that both the neoclassical conductivity and the bootstrap current can change the current profiles substantially. It indicates the importance of the self-consistent calculation of neoclassical equilibria. Self-consistent calculation also makes it possible to analyze the neoclassical current effects on MHD stability. The code can be applied to equilibrium and stability analysis of tokamak plasmas with non-ohmic currents and with neoclassical current effects.

Acknowledgements

The authors would like to thank Drs. J. Manickam and M. Okabayashi at Princeton Plasma Physics Laboratory for interesting and stimulating suggestions. They are also grateful to Dr. M. Tanaka for his continuing encouragement. One of the authors (S.T.) would like to thank Prof. J. D. Callen and Dr. Y. B. Kim at University of Wisconsin for their useful advice.

5. Summary

A numerical scheme for self-consistent calculations of MHD equilibria specified current sources has been presented. The scheme employs the surface averaged parallel current on computing equilibria instead of the toroidal field function or safety factor. The scheme has been applied to high aspect ratio circular tokamaks with the ohmic current. It has been shown that both the neoclassical conductivity and the bootstrap current can change the current profiles substantially. It indicates the importance of the self-consistent calculation of neoclassical equilibria. Self-consistent calculation also makes it possible to analyze the neoclassical current effects on MHD stability. The code can be applied to equilibrium and stability analysis of tokamak plasmas with non-ohmic currents and with neoclassical current effects.

Acknowledgements

The authors would like to thank Drs. J. Manickam and M. Okabayashi at Princeton Plasma Physics Laboratory for interesting and stimulating suggestions. They are also grateful to Dr. M. Tanaka for his continuing encouragement. One of the authors (S.T.) would like to thank Prof. J. D. Callen and Dr. Y. B. Kim at University of Wisconsin for their useful advice.

References

[1] J.D. Callen and R.A. Dory, Phys. Fluids, **15**, 1523 (1972).

[2] K. Lackner, Comput. Phys. Commun. **12**, 33 (1976).

[3] J.L. Johnson, H.E. Dalhed, J.M. Green, R.C. Grim, Y.Y. Hsieh, S.C. Jardin, J. Manickam, M. Okabayashi, R.G. Storer, A.M.M. Todd, D.E. Voss and K.E. Weimer, PPPL-1463, 1978.

[4] J. Delucia, S.C. Jardin and A.M.M. Todd, J. Computational Phys. **37**, 183 (1980).

[5] H.P. Zehrfeld and F. Casci, Comp. Phys. Commun. **31**, 155 (1984).

[6] T.Tsunematsu, S.Tokuda, T. Nemoto, M. Azumi and T. Takeda, Japan Atomic Energy Research Institute Report JAERI-M 86-172, 1986.

[7] R.A. Dory and Y.K.M. Peng, Nucl. Fusion **17**, 1 (1977).

[8] L.L. Lao, H. St. John, R.D. Stambaugh, A.G. Kellman, W. Pfeiffer, Nucl. Fusion **25**, 1575 (1985).

[9] F.L. Hinton and R.D. Hazeltine, Rev. Mod. Phys. **42**, 239 (1976).

[10] S.P. Hirshman and D.J. Sigmar, Nuclear Fusion **21**, 1079 (1981).

[11] Y.B. Kim, University of Wisconsin Plasma Report UWPR **88-2** (1988).

[12] M.C. Zarnstorff, M.G. Bell, M. Bitter, R.J. Goldston,B. Grek et al., Phys. Rev. Letters **60**, 1306 (1988).

[13] Y.B. Kim, J.D. Callen and H. Hamnén, JET-R(88)02 (1988).

[14] J.W. Connor and J.G. Cordey, Nucl. Fusion **14**, 185 (1974).

[15] N. J. Fisch, Rev. Mod. Phys. **59**, 175 (1987).

[16] K. C. Shaing, Plasma Phys. and Controlled Fusion **29**, 1637 (1987).

[17] S.P. Hirshman, Phys. Fluids **21**, 1295 (1978).

[18] S.P. Hirshman and S.C. Jardin, Phys. Fluids **22**, 731, (1979).

[19] D.A. Ehst, K. Evans,Jr. and D.W. Ignat, Nucl. Fusion **26**, 461 (1986).

[20] E.C. Crume,Jr., C.O. Beasley, Jr., S.P. Hirshman and W.I. van Rij, Phys. Fluids **30**, 1152 (1987).

[21] R.W. Hockney, in Method in Computational Physics, Vol.9, Academic Press, New York, 1970, p.135

[22] L.S. Solove'v, JETP **26**, 400 (1968).

Table 1 (a) Friction matrix elements for electrons and ions.

(b) Matrices K^B, K^P and K^{PS} for electrons.

(c) Matrices K^B, K^P and K^{PS} for ions.

(a)

	e	i
l_{11}	Z_I	$-Z_I$
l_{12}	$3Z_I/2$	$-3Z_I/2$
l_{21}	$3Z_I/2$	0
l_{22}	$\sqrt{2}+13Z_I/4$	$\sqrt{2}$

for electrons

(b)

collisionality	K^B	K^P	K^{PS}
K_{11}	$0.53 + Z_I$	3.54	$(3.02+4.25Z_I)/D$
K_{12}	$0.71 + Z_I$	10.63	$(12.43+20.13Z_I)/D$
K_{22}	$1.59+2Z_I$	42.54	$(58.65+101.06Z_I)/D$

$D = 2.23 + 5.32Z_I + 2.40Z_I^2$

for ions

(c)

collisionality	K^B	K^P	K^{PS}
K_{11}	0.53	3.54	3.02/2.23
K_{12}	0.71	10.63	12.43/2.23
K_{22}	1.59	42.54	58.65/2.23

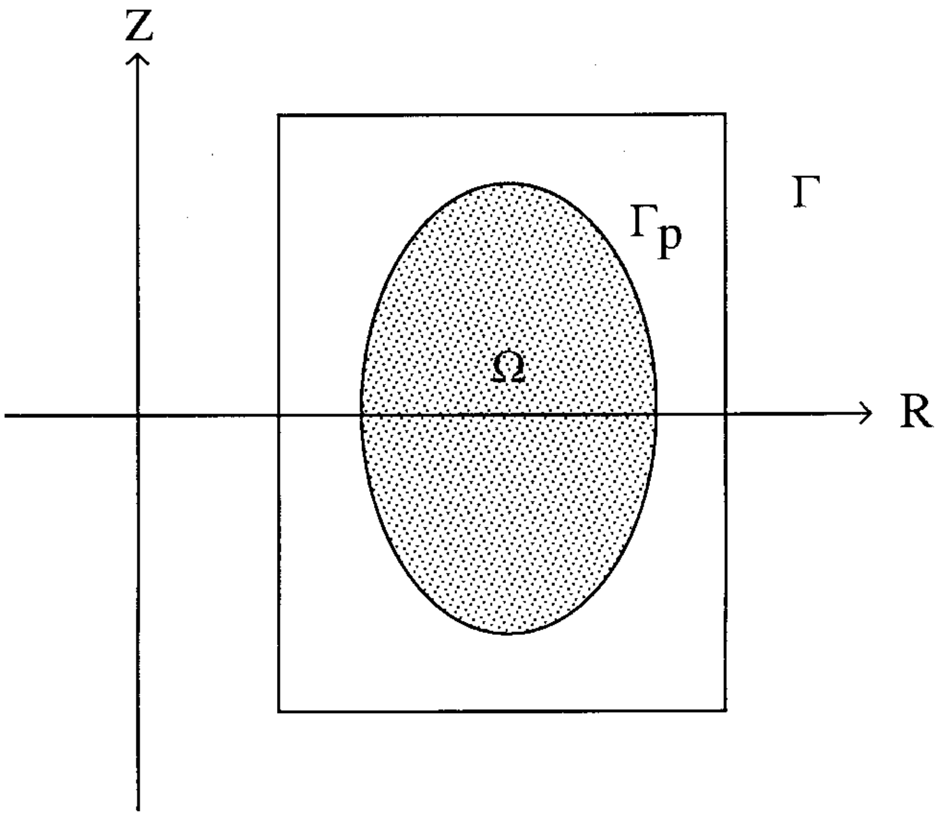

Fig.1 Computational box containing plasma (Ω). Boundary values on Γ are loaded by applying Green's theorem along the plasma surface Γ_p.

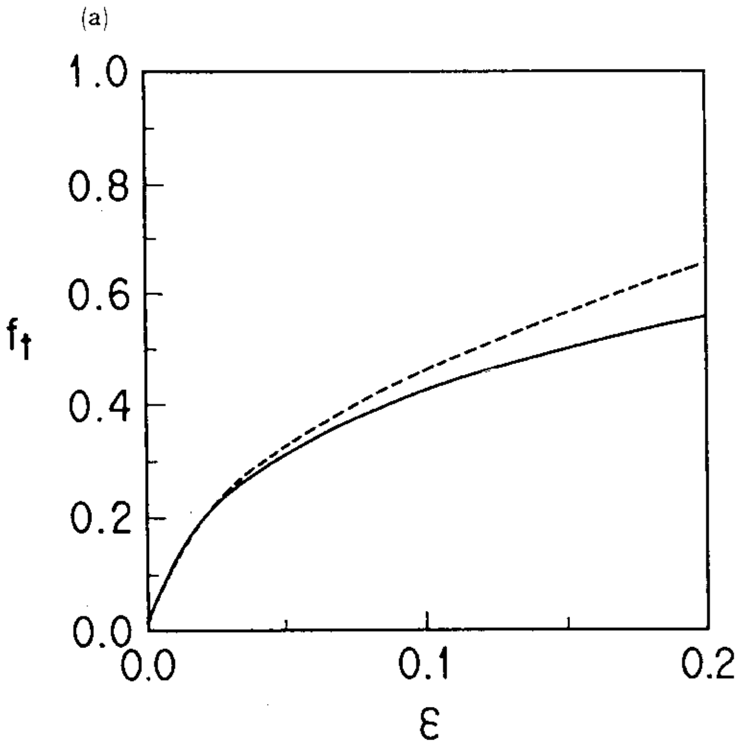

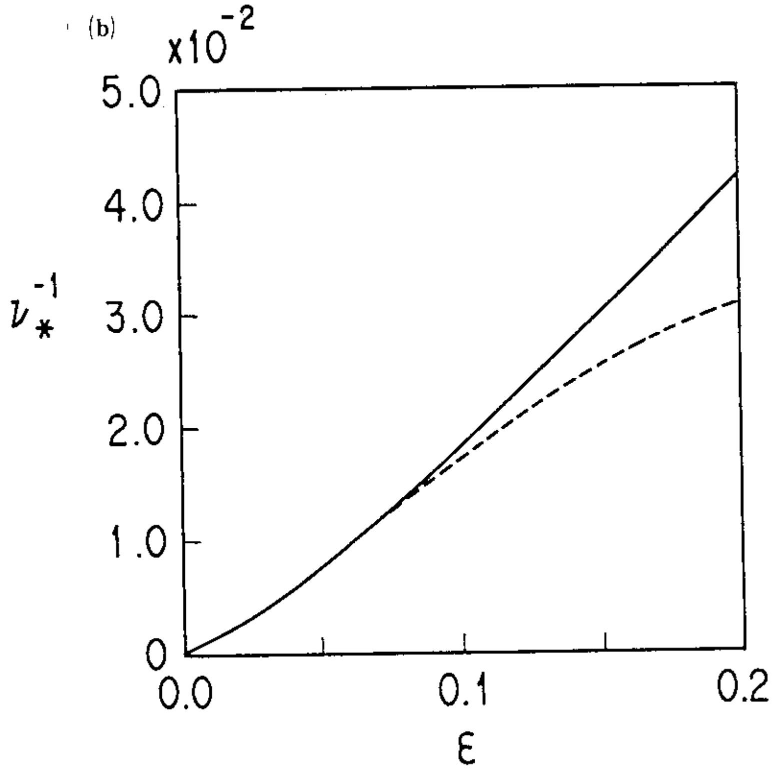

Fig.2 Fraction of trapped particles f_t (a) and collisionality parameter $\nu *^{-1}$ (b) for a high aspect ratio circular tokamak (HARCT) computed from the code (solid lines) and from HARCT limit, eqs.(28) and (29) (dotted line).

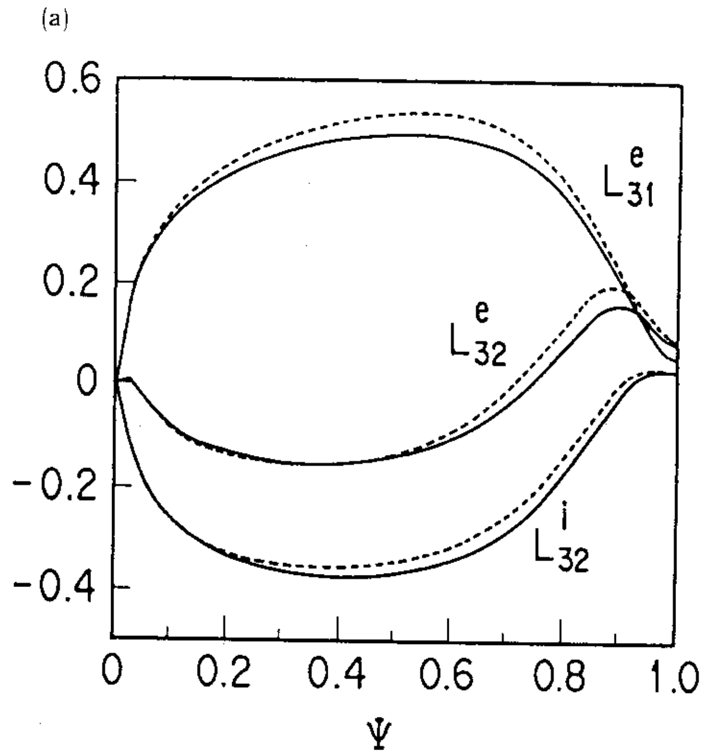

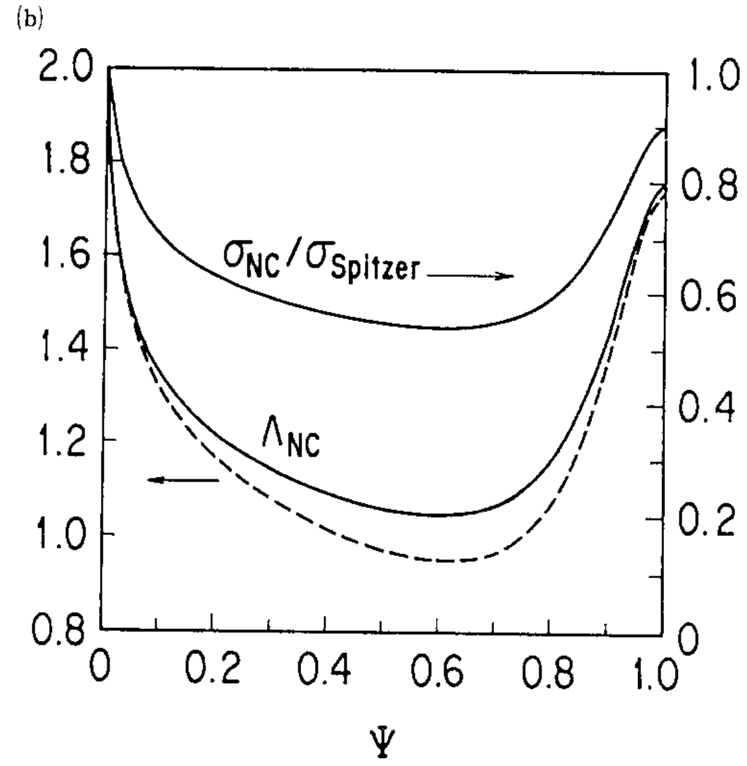

Fig.3 Neoclassical current coefficients for HARCT obtained form the code (solid lines) and form the HARCT limit (dotted lines).

(a) Bootstrap current coefficients $L^e{}_{31}$, $L^e{}_{32}$ and $L^i{}_{32}$.

(b) Neoclassical conductivity coefficient Λ_{NC} and $\sigma_{NC}/\sigma_{Spitzer}$.

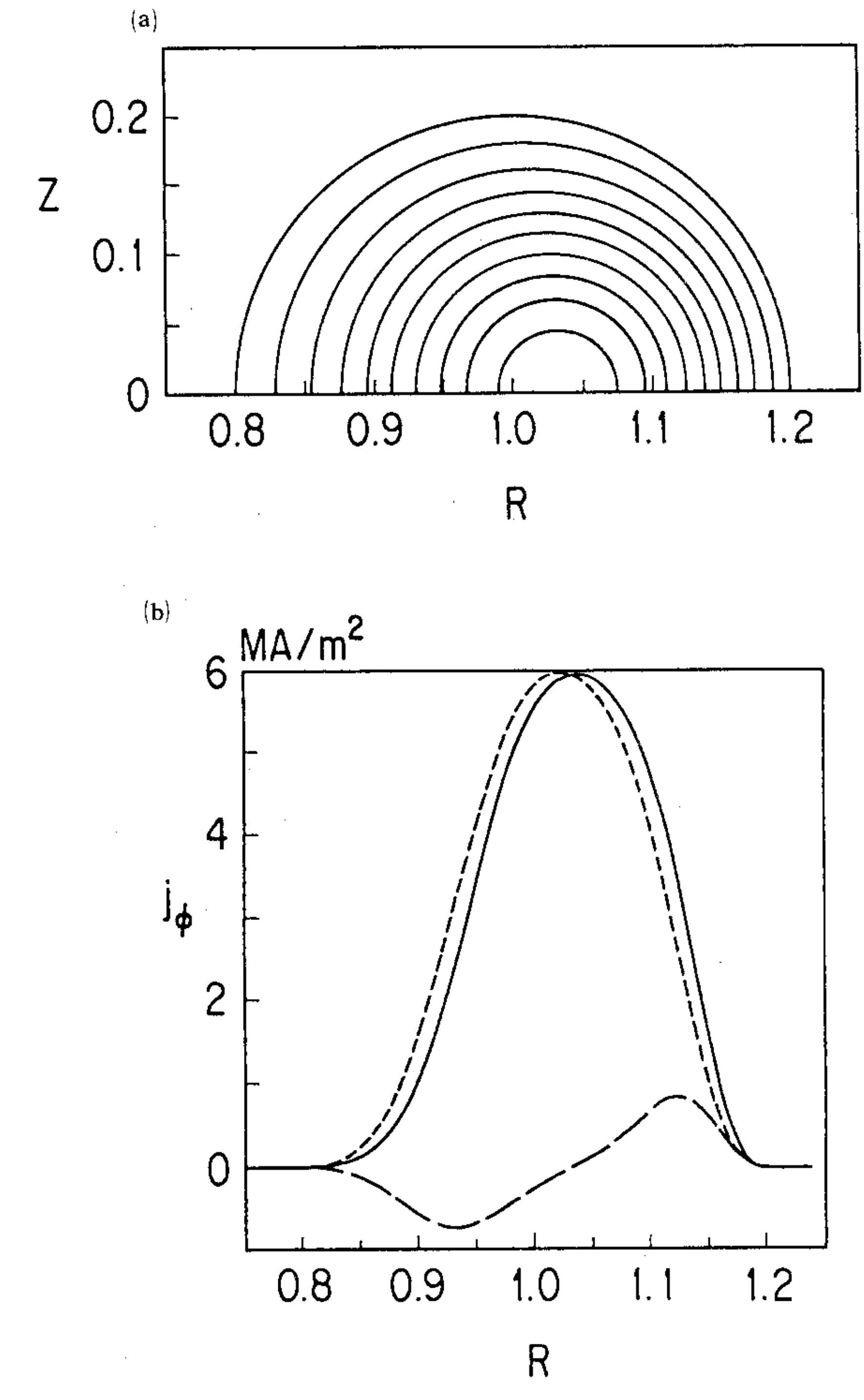

Fig.4 Equilibtium with no neoclassical current effects (classical equilibrium).

(a) Contour lines of poloidal flux function ψ. ψ_{axis} = -4.15×10^{-2}*weber*.

(b) Toroidal currents in the midplane (Z = 0). Solid line is for total current, dotted line for ohmic current and dashed line for pressure current composed of Pfirsh-Schüter current and diamagnetic current.

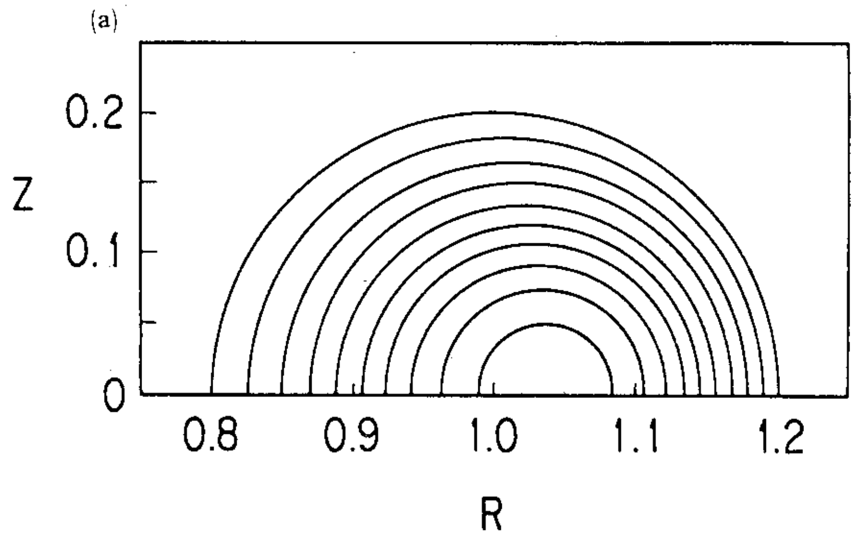

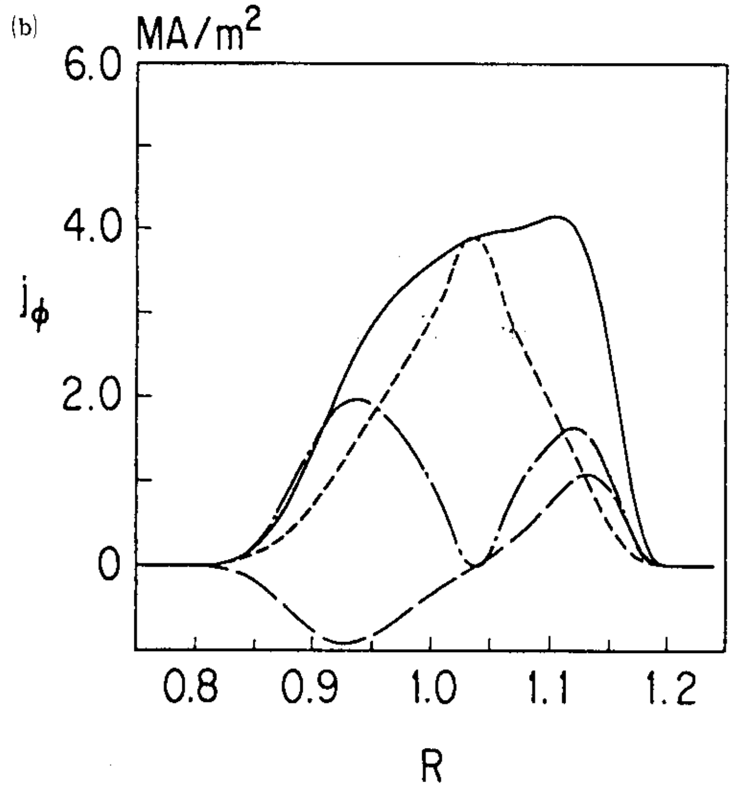

Fig.5 Equilibrium with neoclassical effects (neoclassical equilibrium).

(a) Contour lines of poloidal flux function ψ. ψ_{axis} = -3.54×10^{-2} *weber*.

(b) Toroidal currents in the midplane. Solid line is for total current, dotted line for ohmic current, dashed line for pressure current and dot-dashed line for bootstrap current.

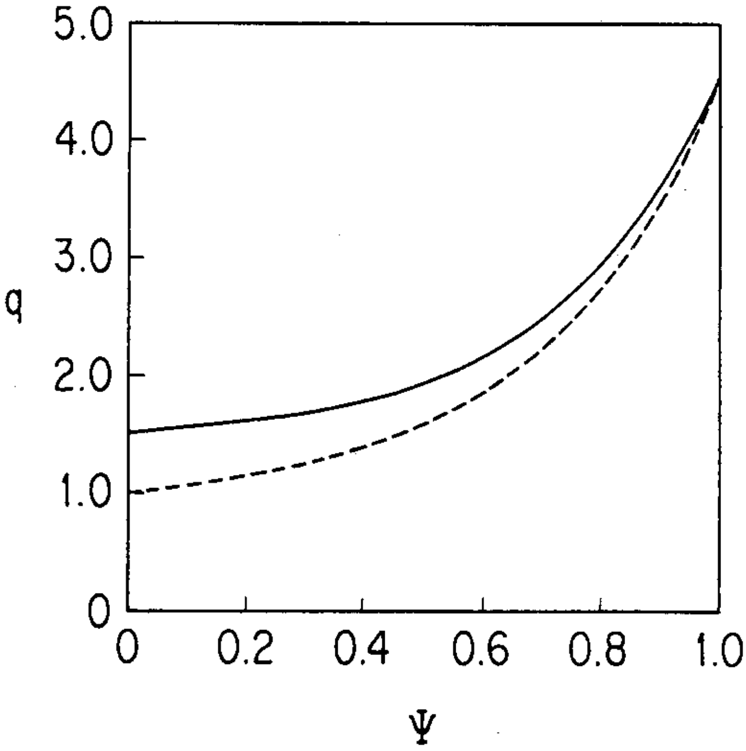

Fig.6 Safety factor q for the neoclassical equilibrium (solid line) and the classical equilibrium (dotted line).